

Apatite formation on poly(2-hydroxyethyl methacrylate)-silica hybrids prepared by sol-gel process

RICARDO O. R. COSTA¹, MARIVALDA M. PEREIRA^{2,*}, FERNANDO S. LAMEIRAS¹, WANDER L. VASCONCELOS²

¹*Centro de Desenvolvimento da Tecnologia Nuclear—CDTN/CNEN—Rua Prof. Mário Werneck, Campus da UFMG, Belo Horizonte, MG, Brazil, 30123-970*

²*Departamento de Engenharia Metalúrgica e de Materiais, Universidade Federal de Minas Gerais, Rua Espírito Santo, 35, Belo Horizonte, MG, Brazil, 30160-030*
E-mail: mpereira@demet.ufmg.br

Hybrids of poly(2-hydroxyethyl methacrylate) (PHEMA), a polymer that has been employed in a wide variety of biomedical applications, and silica-gel, which exhibits a well-known bioactivity, were produced. The obtained hybrids were characterized and their *in vitro* ability to induce the formation of a calcium phosphate layer on the surface was evaluated. The surface area of hybrids decreased with increasing amounts of PHEMA so that hybrids with more than ~40% PHEMA are virtually non-porous. All hybrids induced the formation of a calcium phosphate layer on their surfaces when soaked into simulated body fluid. The induction time and the morphology of the apatite layer varied according to the polymer content.

© 2005 Springer Science + Business Media, Inc.

1. Introduction

The possibility of manufacturing ceramics with high degree of purity at low temperatures via sol-gel process [1] made feasible the incorporation of an organic moiety into the ceramic structure with integration at the nanometer level [2]. Since the mid-1980s, when the first sol-gel derived hybrids were obtained by mixing linear polymer chains with silica precursors [3–5], many works have been conducted trying to probe structure and to explore potential applications of this type of materials, as demonstrated by several review papers [2, 6–10].

The incorporation of polymeric components to sol-gel derived materials may constitute an important tool to either enhance mechanical properties [5, 6, 11–13] or provide more compatible media for encapsulation of biological molecules and medicines [14, 15]. Therefore, room exists for development of lightweight structural organic-inorganic hybrids with high toughness and bone-like elastic modulus, as well as hybrids for other biomedical applications, including biocatalysts, biosensors, immunodiagnostics and drug delivery systems.

A wide variety of types of organic polymers have been employed in the syntheses of hybrids of silica [2, 16]. The type of polymer employed is one of the main features affecting structure and properties of hybrids because they depend essentially on chemical in-

teractions established between organic and inorganic moieties. Particularly the polymer poly(2-hydroxyethyl methacrylate) (PHEMA) is an interesting choice because, in addition to being easily soluble in the water-alcohol mixtures employed in sol-gel method, its pendant hydroxyl groups lead to the formation of hydrogen bonds and eventual condensation with silanol groups [17–20], thus favoring the production of structurally homogeneous materials within a wide range of compositions [21]. Moreover, PHEMA has been employed in a wide variety of biomedical applications, featuring as highly biocompatible [22–26] among the non-biodegradable polymers.

The potential bioactivity of PHEMA-silica hybrids [27], as well as of poly(methyl methacrylate)-silica [28] and poly(dimethylsiloxane)-silica hybrids [29], has been reported. *In vitro* tests have demonstrated the induction of an apatite layer on surface of these materials when soaked into simulated body fluid (SBF) [30], but only in samples with addition of calcium to the network structure. Nevertheless, studies performed by Hench and coworkers involving bioactive glasses [31] and silica gel [32] have shown that silica dissolution and Si-OH formation play an important role on the mechanism of apatite precipitation. While dense glasses with more than 60% silica are not bioactive, pure silica gel exhibits bioactivity probably due to large surface area and high silanol concentration on the surface, which

*Author to whom all correspondence should be addressed.

are believed to increase the apatite nucleation rate. It has also been demonstrated that the increase in pore volume in samples treated at 600 °C accelerates apatite deposition. It has been suggested that pores larger than ~1.6 nm are privileged nucleation sites due to the enhanced ionic activity and absence of diffusion limiting effects [32].

Porous PHEMA-silica hybrids with controlled surface areas can be produced by combining the components at the desired proportions. This work aims to obtain PHEMA-silica hybrids, to determine if they induce apatite precipitation and to evaluate the effects of pore volume and size on induction time for apatite nucleation.

2. Experimental

2.1. Synthesis of hybrids

The procedure for the synthesis of hybrids has been adapted from previous studies by our group [21]. In a first step, PHEMA was synthesized under N₂ by dissolving 3.8 mL (30.4 mmol) of the monomer 2-hydroxyethyl methacrylate (HEMA) (99% Polysciences) and 20.0 mg (0.121 mmol) of the initiator 2,2'-azobis(isobutyronitrile) (AIBN) (98% Polysciences) in 20.0 mL of ethanol (99.8% Merck). The sealed reacting flask was heated to (70.0 ± 0.2) °C for 24 h. Then, the polymer solution was cooled to room temperature and used for the syntheses of hybrids.

Hybrids were obtained by mixing varied amounts of polymer solution with 4.0 mL of tetramethoxysilane (TMOS) (98% Aldrich) and 2.0 mL of deionized water, which corresponds to a water: TMOS mol ratio of ~4. Silica was synthesized under similar reaction conditions for the purpose of comparison. No acidic or basic catalyst was added. Additional amounts of ethanol were employed to dilute PHEMA solution before the addition of silica precursors so as to provide a homogeneous reacting mixture. Ethanol volumes added were calculated so that each precursor solution contained a total of ~8.0 mL of ethanol, considering 100% conversion of HEMA. TMOS volume to PHEMA mass ratios selected so as to obtain hybrids with different pore surface areas. Table I specifies the synthesis conditions of each one of the produced hybrids, which were termed HMx

TABLE I Reaction conditions for the syntheses of hybrids

Reagents	Silica	HM25	HM10	HM7	HM5	HM4
PHEMA solution (g)	0	0.80	2.00	2.86	4.00	5.00
Additional ethanol (mL) ^a	8.0	7.2	6.0	5.1	3.9	2.9
TMOS (mL)	4.0	4.0	4.0	4.0	4.0	4.0
Water (mL)	2.0	2.0	2.0	2.0	2.0	2.0
TMOS (mL) to PHEMA (g) ^b	∞	25	10	7	5	4
Nominal % PHEMA ^c	0	9.0	19.9	26.1	33.1	38.2

^aCalculated so as to give a total volume of 8.0 mL of ethanol added, assuming 100% of monomer conversion.

^bExpected ratio, assuming 100% of monomer conversion.

^cTheoretical polymer contents expected, calculated considering only PHEMA and dry silica, assuming total conversion of TMOS into SiO₂, without remaining free water molecules, silanol or alcoxide groups. 1.00 g of TMOS is theoretically converted to 0.3047 g of SiO₂.

according to the ratio “x” of TMOS to PHEMA employed. Nominal polymer contents, ranging from 0 wt% to ~38 wt%, were calculated considering only PHEMA and dry silica, assuming total conversion of TMOS into SiO₂.

After stirring for 30 min, each solution was transferred to 4 cylindrical flasks, which were sealed and maintained at room temperature for 4 days, time enough for gelation. The samples were then aged at 60 °C for 38 h and finally dried for 48 h at 60 °C and for 24 h at 100 °C.

2.2. In vitro studies in SBF

A SBF solution was prepared according to Kokubo *et al.* [30]. Hybrid samples with dimensions 5 × 5 × 3 mm had their surfaces smoothed with sand paper #1000 and were suspended in the SBF solution at 37 °C by a nylon string. The ratio of geometric surface area (SA) to solution volume (V) was fixed at 0.1 cm⁻¹. The specimens were soaked for various times during which SBF was not changed. They were then removed from solution, excess water was gently removed by tissue paper followed by drying in air.

2.3. Characterization

Nitrogen sorption analyses (Quantachrome Autosorb-1) of the obtained hybrids were performed by crushing the samples into small pieces (<1 mm) and degassing at 110 °C for at least 12 h. Surface areas (*S_p*) and pore size distributions were then calculated from the adsorption-desorption isotherms. Fourier transform infrared (FTIR) spectra were recorded (Perkin Elmer FT-IR Spectrometer Spectrum 1000). Hybrids surfaces before and after soaking monoliths into SBF were analyzed using a diffuse reflectance apparatus. Bulk of hybrid samples were also analyzed by crushing into powder and using small amounts of sample placed on an aluminum-coated abrasive pad. PHEMA film was obtained after solvent removal by drying and analyzed using an attenuated total reflection apparatus. Scanning electron microscopy (SEM) images of samples were obtained on a JEOL JSM-840A.

3. Results and discussion

FTIR spectra obtained for PHEMA film, hybrids and silica powders are compared in Fig. 1. PHEMA spectrum exhibits typical absorption bands, including a strong peak at 1715 cm⁻¹, assigned to C=O, and the broad band at 3035–3680 cm⁻¹, corresponding to O–H vibrations of side groups [17, 18, 23]. It is possible to notice the increase in polymer content in hybrids produced with decreasing TMOS volume to PHEMA mass ratio (cf. Table I). The peak at 1715 cm⁻¹ as well as other peaks assigned to polymer groups in the regions 2880–2950 and 1380–1480 cm⁻¹ arise in spectrum of hybrid HM25 and increase in intensity comparatively to the peak at 1630 cm⁻¹, which corresponds to free H₂O in porous structure. The larger amplitude bands of silica gel in the region 800–1200 cm⁻¹ (Fig. 2(a)) obscure the fingerprint region.

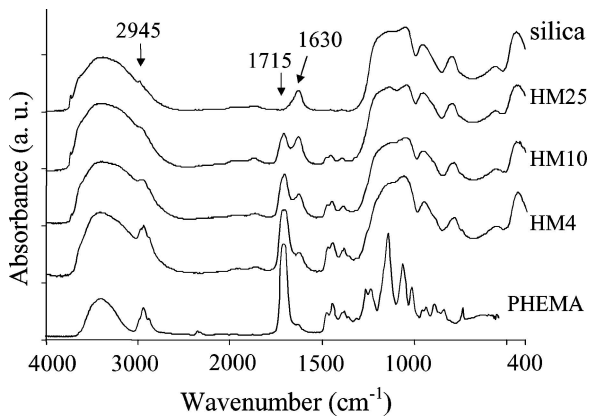


Figure 1 FTIR spectra of polymer PHEMA and bulk of silica, hybrids HM25, HM10, HM4, obtained from PHEMA film and powdered samples.

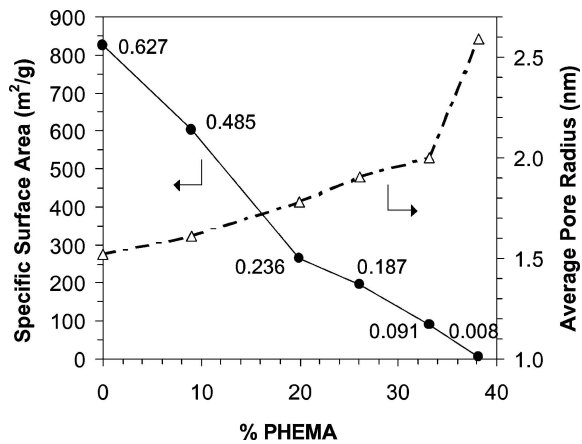


Figure 2 Dependence of specific pore surface area and average pore radius on nominal polymer content in hybrids (cf. Table I). Numbers are specific pore volumes in cm³/g. Errors are within 5%.

From nitrogen sorption analyses, pore radius and surface area were determined for the obtained silica and hybrids. Fig. 2 shows the influence of the nominal polymer content on textural properties of hybrids. While silica gel synthesized under similar reaction conditions has a pore surface area as high as 826 m²/g, increasing amounts of PHEMA in the hybrids decrease continuously their surface areas down to 6 m²/g for hybrid HM4. Pore volumes also decrease (numbers in Fig. 2) so that hybrids with more than ~40% PHEMA are virtually non-porous. On the other hand, the average pore

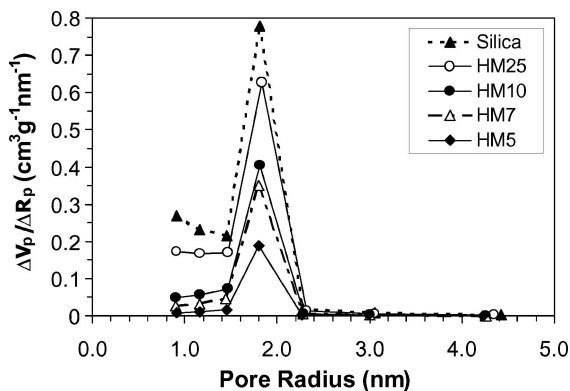


Figure 3 Comparison of pore radius distributions in silica and hybrids HM25, HM10, HM7, HM5 with increasing polymer content.

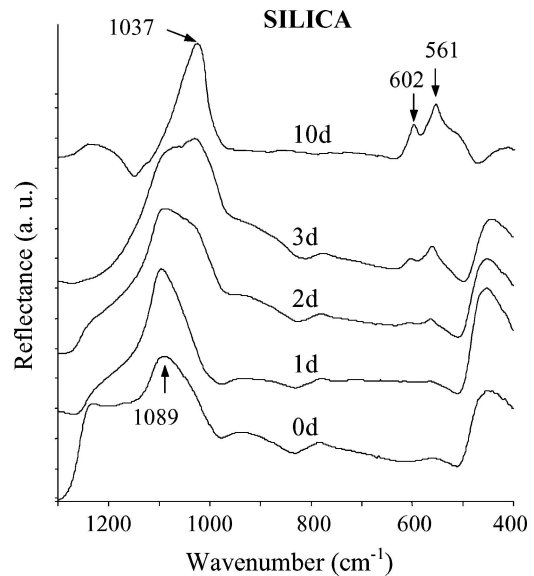


Figure 4 FTIR spectra of silica surface before and after soaking into SBF for 1, 2, 3 and 10 days.

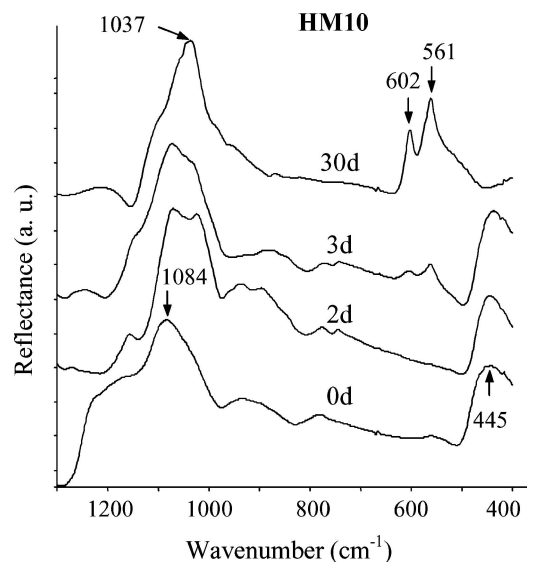


Figure 5 FTIR spectra of surface of hybrid HM10 before and after soaking into SBF for 2, 3 and 30 days.

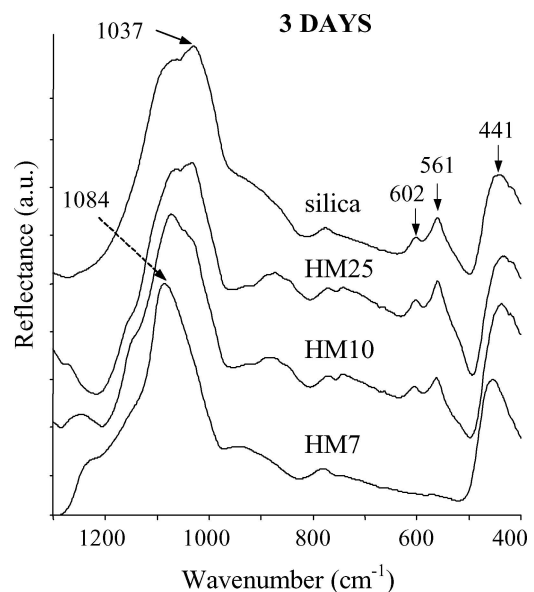


Figure 6 FTIR spectra of surfaces of silica and hybrids HM25, HM10 and HM7 after soaking into SBF for 3 days.

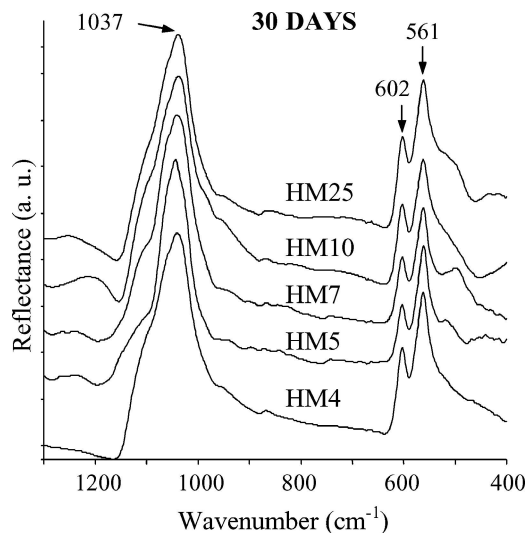


Figure 7 FTIR spectra of surfaces of hybrids HM25, HM10, HM7, HM5 and HM4 after soaking into SBF for 30 days.

radius increases with PHEMA content from 1.5 nm for pure silica to only 2.6 nm for hybrid with 38% PHEMA.

The decrease in pore surface area takes place due to the fact that, differently from the solvent, which evaporates and leaves voids during drying step, polymer chains remain either inside the pores or blocking their entrance. The dependence of pore surface area on PHEMA content is useful for producing hybrids with controlled surface areas by simply changing PHEMA concentration in the initial reacting solution. While sil-

ica nanoparticles are condensed to form silica network, solvent and polymer chains are excluded to the regions that will constitute the pore structure after drying, provided that these molecules do not take part in condensation reactions. When polymer content is increased, it is expected a tendency for increase in size of polymer domains, accompanied by the local presence of larger amounts of solvent, whose further evaporation upon drying will possibly generate hybrids with larger pore sizes. Additional considerations can be made by looking at Fig. 3, which presents pore size distributions for silica and hybrids HM25, HM10, HM7 and HM5. The decrease in pore volume with addition of polymer becomes evident by comparing the progressively lower micro and mesopore volumes in hybrids with larger PHEMA contents. The increase in average pore size apparently comes from the elimination of micropores concomitantly with the fact that the average size of mesopores seems to remain unaffected.

Figs. 4 and 5 illustrates the FTIR spectra for pure silica gels and hybrid HM10 respectively before and after immersion in SBF for different time periods. The bands at 561 and 602 cm^{-1} , which can be ascribed to P–O bending vibration, and at 1037 cm^{-1} , ascribed as P–O stretching vibration [31], demonstrate the formation of a low crystallinity hydroxyapatite (HA) layer on the surface of both pure silica and the hybrid material upon immersion in SBF. The induction time for apatite formation on the hybrid material was higher than for pure silica. All hybrids induced the formation of the HA layer on their surfaces when soaked into SBF, as

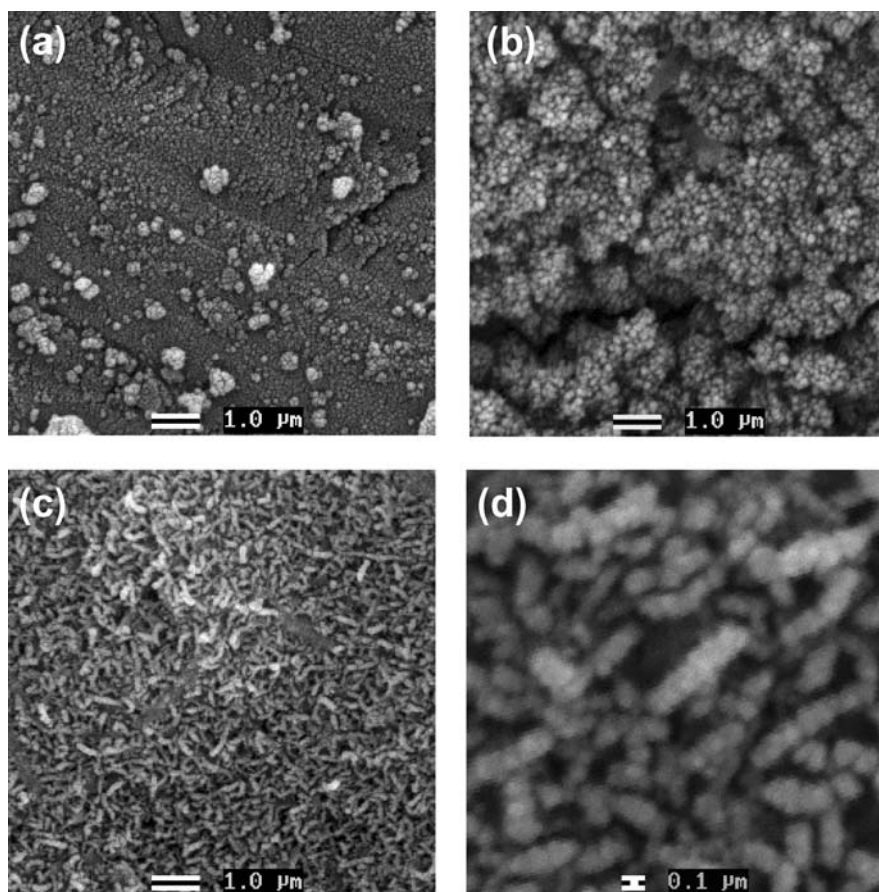


Figure 8 SEM images of surfaces of hybrid HM10 as synthesized (a) and after soaking into SBF for 3 days (b) and 30 days (c,d). Magnifications are 10,000X for images (a), (b) and (c) and 50,000X for image (d).

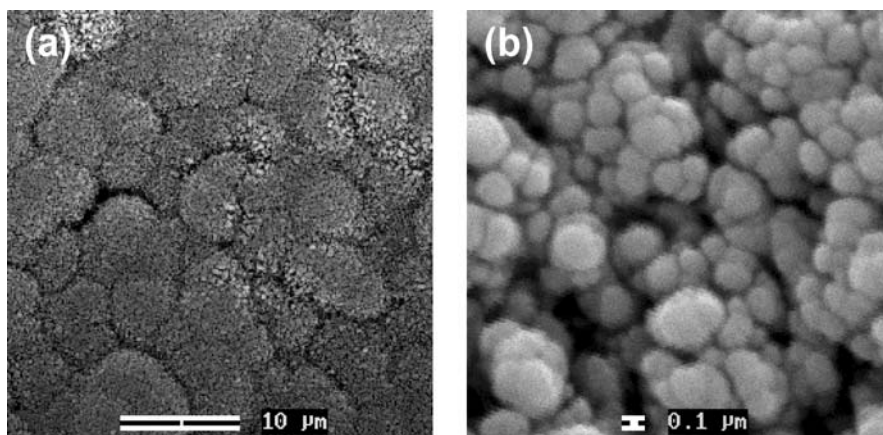


Figure 9 SEM images of surface of hybrid HM7 after soaking into SBF for 30 days with magnifications of 2,500X (a) and 50,000X (b).

shown in Figs. 6 and 7. However the induction time increased with increasing polymer content, from 2 days for pure silica and HM25, to 3 days for HM10 and approximately 30 days for HM5 and HM4.

It should be noted that the immersion procedure used in this study used a fixed geometric SA/V ratio, similar to other studies on sol-gel derived materials [36]. If the total SA/V ratio was considered a larger solution volume would be used in the *in vitro* experiments. Also, the SBF solution was not changed during the experiments. Both conditions used here are less favorable to the growth of an apatite layer on the surface of the silica/PHEMA hybrids. Changing these conditions would increase the amount of calcium and phosphate ions available for apatite growth and probably increase the thickness of the layer formed and affect the induction times measured.

The increase in the apatite nucleation time is directly related to the large decrease in surface area and pore volume as the polymer content increased. The more widely accepted model describes the kinetics of HA precipitation on silica glasses as being a function of the concentration of Si—OH groups, presumably nucleation sites for HA [32]. The increase in induction time for HA precipitation with the decrease in S_p of hybrids observed in this work may be attributed to the decrease in the amount of silanol groups available for apatite nucleation in accordance with this model. Considerations involving pore size in this case seem to be of minor importance, since R_p increases with PHEMA content. These results are in agreement with previous observations on sol-gel derived ceramics and also on other hybrid systems [32–34]

Fig. 8 presents SEM images of the surface of hybrid HM10 after immersion in SBF for 3 and 30 days. After immersion in SBF for 3 days the irregular aspect of the surface produced by the grinding preparation procedure used is still observed. The apatite nucleus detected by FTIR are not clearly distinguished on the surface. After 30 days immersion an apatite layer is present covering the surface. Fig. 9 shows the apatite layer formed on hybrid HM7 after 30 days immersion. A different morphology is observed depending on the polymer content in the hybrids. The variation in morphology was also observed for silica gel-glasses with different pore structure [35].

4. Conclusions

Homogeneous, transparent monoliths of PHEMA-SiO₂ hybrids were successfully obtained by the sol-gel process. The surface area of hybrids decreased with increasing amounts of PHEMA so that hybrids with more than ~40% PHEMA are virtually non-porous. All hybrids induced the formation of a calcium phosphate layer on their surfaces when soaked into simulated body fluid. The induction time and the morphology of the apatite layer varied according to the polymer content. An increase in induction time for HA precipitation was observed with increasing polymer content, and was attributed to the decrease surface area and consequent decrease in the amount of silanol groups available for apatite nucleation.

Acknowledgments

The authors gratefully acknowledge FAPEMIG, CNPq and CAPES for the financial support. RORC also thanks Max P. Ferreira (CDTN), for gently offering his lab for partial development of this study, and Ney P. Sampaio (Dept. of Physics—UFMG), for his kind collaboration on acquirement of SEM images.

References

1. C. J. BRINKER and G. W. SCHERER, "Sol-Gel Science: The Physics and Chemistry of Sol-Gel Processing" (Academic Press, 1990).
2. J. WEN and G. L. WILKES, *Chem. Mater.* **8** (1996) 1667.
3. J. E. MARK, C. Y. JIANG and M. Y. TANG, *Macromolecules* **17** (1984) 2613.
4. H. H. HUANG, B. ORLER and G. L. WILKES, *Polym. Bull.* **14** (1985) 557.
5. E. J. A. POPE, M. ASAMI and J. D. MACKENZIE, *J. Mater. Res.* **4** (1989) 1018.
6. B. M. NOVAK, *Adv. Mater.* **5** (1993) 442.
7. L. MASCIA, *Trends Polym. Sci.* **3** (1995) 61.
8. P. JUDEINSTEIN and C. SANCHEZ, *J. Mater. Chem.* **6** (1996) 511.
9. A. B. WOJCIK and L. C. KLEIN, *Appl. Organometal. Chem.* **11** (1997) 129.
10. Y. CHUJO and R. TAMAKI, *MRS Bull.* **26** (2001) 389.
11. B. ABRAMOFF and L. C. KLEIN, in "Ultrastructure Processing of Advanced Materials," edited by D. R. Uhlmann and D. R. Ulrich (Wiley, 1992) p. 401.
12. S. YANO, K. NAKAMURA, M. KODOMARI and N. YANAUCHI, *J. Appl. Polym. Sci.* **54** (1994) 163.
13. M. KAMITAKAHARA, M. KAWASHITA and N. MIYATA, *J. Sol-Gel Sci. Tech.* **21** (2001) 75.

14. GILL and A. BALLESTEROS, *J. Am. Chem. Soc.* **120** (1998) 8587.
15. D. AVNIR, S. BRAUN, O. LEV and M. OTTOLENGHI, *Chem. Mater.* **6** (1994) 1605.
16. A. B. BRENNAN and T. M. MILLER, in "Kirk-Othmer Encyclopaedia of Chemical Technology" (Wiley, 1994) p. 644.
17. P. BOSCH, F. DEL MONTE, J. L. MATEO and D. LEVY, *J. Polym. Sci. A Polym. Chem.* **34** (1996) 3289.
18. Z. H. HUANG and K. Y. QIU, *Polymer* **38** (1997) 521.
19. Y. WEI, D. JIN and C. YANG, *Mat. Sci. Eng. C* **6** (1998) 91.
20. P. HAJJI, L. DAVID and J. F. GERARD, *J. Polym. Sci. B Polym. Phys.* **37** (1999) 3172.
21. R. O. R. COSTA and W. L. VASCONCELOS, *J. Non-Cryst. Sol.* **304** (2002) 84.
22. T. D. DZIUBLA, M. C. TORJMAN and J. I. JOSEPH, *Biomaterials* **22** (2001) 2893.
23. D. KLEE and H. HÖCKER, *Adv. Polym. Sci.* **149** (2000) 1.
24. I. RAVAGLIOLI and A. KRAJEWSKI, in *Bioceramics* (Chapman & Hall, 1992).
25. J. P. MONTEHÉARD, M. CHATZOPOULOS and D. CHAPPARD, *J. Macromol. Sci. Macromol. Rev.* **32** (1992) 1.
26. F. O. ESCHBACH and S. J. HUANG, in "Interpenetrating Polymer Networks," edited by D. Klemperer, L. H. Sperling and L. A. Utracki, *Adv Chem Series* (1990) vol. 239, p. 205.
27. C. OHTSUKI, T. MIYAZAKI and M. TANIHARA, *Key Eng. Mater.* **192–195** (2001) 39.
28. S. M. JONES, S. E. FRIBERG and J. SJÖBLOM, *J. Mater. Sci.* **29** (1994) 4075.
29. K. TSURU, C. OHTSUKI and A. OSAKA, *J. Mater. Sci. Mater. Med.* **8** (1997) 157.
30. T. KOKUBO, H. KUSHITANI, S. SAKKA et al., *J. Biomed. Mater. Res.* **24** (1990) 721.
31. L. L. HENCH and Ö. ANDERSSON, in "An Introduction to Bioceramics," edited by L. L. Hench and J. Wilson (World Scientific, 1993) p. 41.
32. M. M. PEREIRA, A. E. CLARK and L. L. HENCH, *J. Am. Ceram. Soc.* **78** (1995) 2463.
33. Q. CHEN, N. MIYATA, T. KOKUBO and T. NAKAMURA, *J. Biomed. Mater. Res.* **51** (2000) 605.
34. N. MIYATA, K. FUKU, Q. CHEN, M. KAWASHITA, T. KOKUBO and T. NAKAMURA, *Biomaterials* **23** (2002) 3033.
35. M. M. PEREIRA, *Cerâmica* **42** (1996) 731.

*Received 27 February 2004
and accepted 18 November 2004*